ACCEPTED MANUSCRIPT

On Demand Manipulation of Ferrofluid Droplets by Magnetic Fields

A. Ray[1], V. B. Varma[1], P. J. Jayaneel[2], N. M. Sudharsan[2],

Z. P. Wang[3] and R. V. Ramanujan[1] *

[1]School of Materials Science and Engineering, Nanyang Technological University, Singapore, 639798

[2]Department of Mechanical Engineering, Rajalakshmi Engineering College, Chennai, India, 602105

[3]Singapore Institute of Manufacturing Technology, 71 Nanyang Drive, Singapore, 638075

* Corresponding author

Tel: +65 – 6790 4342. Fax: +65 – 6790 9081. E-mail: ramanujan@ntu.edu.sg

Research Highlights

- Facile and controllable manipulation of ferrofluid droplet size by a permanent magnet.
- Droplet merging and generation of larger droplets after merging studied.
- Controllable change in droplet area, droplet area increased by five times.
- Effect of magnetic field intensity, carrier medium viscosity, initial droplet size, flow rates, and flow rate ratio on change in droplet area studied.
- Droplet size change induced by the applied magnetic field is higher for a lower viscosity carrier medium.
- Numerical simulations and experimental results show a similar trend.

Abstract

Magnetic droplets, consisting of magnetic nanoparticles in a carrier fluid, are of high interest due to applications such as remote and wireless control in a microfluidic environment. We investigated the influence of magnetic field on the control of ferrofluid droplet size in a nonmagnetic carrier fluid. Generation of larger droplets by a re-pumping mechanism was studied. The magnetic field leads to coalescence and mixing of the magnetic droplets. A significant response of the ferrofluid droplets to changes in flow rate ratio, the viscosity of the carrier medium and magnetic field intensity was observed.

ACCEPTED MANUSCRIPT

The droplet size can be increased by three times of its initial diameter by tuning the magnetic field intensity. Our modeling results show a similar trend to the experimental findings. Such control, mixing, and re-pumping of droplets is relevant to novel Lab-on-a-Chip applications.

Keywords: Ferrofluid, Droplets, Re-pumping, Actuation, Magnetic field, Viscosity, Coalescence,

1 Introduction

In recent years, multiphase microfluidics has become one of the exciting fields for a variety of research domains such as biomedicine, chemistry, and medicine [1-4]. In microfluidics, mixing and the reaction of two entities becomes challenging when the feature size decreases to the micron scale [5-7]. Droplet-based microfluidics systems have several advantages compared to continuous flow systems on a Lab-on-a-Chip (LoC) platform[8, 9], including manipulation of droplet dimensions [10-13]. The volume of these droplets can range from microliter to picoliter [14], permitting applications such as chemical reactions and mixing at a small scale in a controlled environment [15, 16]. For a droplet-based system, each droplet can be treated as a distinct entity. Various mixing technologies have been previously reported where complex geometrical features were employed [17-19], including curved and zig-zag features. However, fabrication of such geometries is complex and expensive [20].

Apart from studying the effect of complex geometries, active mixing in microfluidics under the influence of external electrical and mechanical forces has also been studied [21]. These forces cause chaotic flow patterns, resulting in mixing. Electrohydrodynamic, electrophoretic and electro-kinetic effects were used to introduce external electric forces; micro stirrer and pressure difference effects were used to generate mechanical forces [22, 23]. However, application of such external forces can induce temperature changes and uncontrolled

ACCEPTED MANUSCRIPT

mechanical forces, which are not desirable for mixing and reaction, respectively. A technology that is wireless, cost effective, affordable, simple to use, which does not generate heat and is insensitive to geometry and size, is required for controlled manipulation in droplet-based microfluidic systems. Hence, the combination of droplet-based microfluidics with external magnetic fields was studied in this work.

Dispersions of ferrimagnetic or ferromagnetic particles in the nano/micron-size range have been studied [24-26] and water-based ferrofluid droplet systems have been investigated [27-30]. Ferrofluids are colloidal suspensions of magnetic nanoparticles, coated with a surfactant, in either a water based or oil based carrier fluid. Surfactants are used to minimize particle aggregation and sedimentation. Such fluids have been extensively used in commercial applications such as sensors, dampers, vacuum technology, lubrication etc [31-33]. In microfluidics, ferrofluids have been used to accomplish actuation of droplet-based systems under the influence of magnetic [34-37]. Such magnetic droplet-based microfluidic systems result in new functionalities, e.g., mixing, droplet fusion, trapping, transport, sorting-separation, pumps, valves, and switches [38-40]. Magnetic fields can be generated using solenoid based systems or permanent magnets.

There is interest in manipulating samples and reagents in isolated and microscale droplets [41, 42]. The manipulation process should be on-demand, easily-monitored and allow multi-step reactions. Such experiments will minimize sample loss, cross contamination and increase mixing and reaction/detection. Although several droplet-based schemes have been developed for transport and fusion [40], splitting [43], sorting [44], and storing [45], it is challenging to merge and trigger a reaction in droplets which contain reagents. On demand manipulation of droplets has been explored using surface modification techniques, complex geometries, application of electric and magnetic fields [27, 41, 42, 46, 47].

ACCEPTED MANUSCRIPT

Hence, to address this challenge, our present work reports the investigation of on demand manipulation of the magnetic droplet-based system in continuous flow under the influence of an external magnetic field. Droplet control was performed by an external magnetic field, droplet merging and release of the larger droplet was observed. A range of flow rate ratios Q, viscosity and magnetic field intensity were studied. The magnetic volume force changes with the volume of the magnetic nanoparticles within the droplet. Experiments were performed with immiscible fluids, primarily with oils (heavy mineral oil and silicone oil) and water-based ferrofluid. Numerical simulations were carried out to model the experimental results. The primary significance of this work is the control of droplet motion, droplet coalescence, mixing and droplet size in an external magnetic field.

2 Materials and Experimental Method

Following subsections describe the materials utilized to perform the experiments, terms, definitions, the experimental methodology used for the generation, merging, and re-pumping of the droplets.

2.1 Materials

For droplet generation, commercial heavy mineral oil and silicone oil were used as the continuous phase (CP) and water-based ferrofluid as the dispersed phase (DP). Properties of the water-based ferrofluid (EMG 807, Ferrotec, Singapore) are 2.0 % (v/v) Fe_3O_4 nanoparticle concentration, 10 nm particle size, 11 mT saturation magnetization and 1.1×10^3 kg/m^3 density (supplier data sheet). The viscosity of the ferrofluid at 27^{o}C is less than 5 mPa s and the initial susceptibility at 25^{o}C is $\chi = 1.88$ (supplier data sheet). Ferrofluid was used as received, without any dilution. The density and dynamic viscosity of the heavy mineral oil (CAS Number: 8042-47-5, Sigma-Aldrich, Singapore) at 25^{o}C are 8.38×10^2 kg/m^3 and 118 mPa.s, respectively. The

ACCEPTED MANUSCRIPT

density and dynamic viscosity of the silicone oil (Catalog Number: KF-96-100CS, Shin-Etsu, Japan) at 25^{o}C are 9.7x 10^{2} kg/m^{3} and 85 mPa.s, respectively.

2.2 Terms and Definitions

The flow focusing geometry which was used for the droplet generation is defined as the 4-junction assembly, which consists of two inlets for the CP, one inlet for the DP and one outlet which is then connected to a microchannel, where droplets are to be generated. Initial ferrofluid droplet size is primarily tuned by controlling the flow rate ratio Q. The flow rate ratio, Q is defined as the ratio of flow rate of the continuous phase of oil (Q_{oil}) to the flow rate of the dispersed phase of ferrofluid (Q_{ff}), viz. $Q=Q_{oil}/Q_{ff}$.

Initial ferrofluid droplets (IFDs) are the droplets generated by the 4-junction assembly by tuning Q in the region x<0, which travels in the positive x direction. Location x=0 mm is the reference position, assigned to the centre of the magnet, which is denoted by the red dotted line in Figure 1b. When a magnetic field is applied, IFDs are seized near x=0 mm and coalesce, resulting in the formation of the coalesced ferrofluid droplet (CFD). The droplets, released from the CFD in the positive x region and whose size is mainly controlled by the applied magnetic field strength (in addition to the flow rate ratio and viscosity), are termed as the final ferrofluid droplets (FFD). The ratio of the FFD diameter (D_{FFD}) to IFD diameter (D_{IFD}) is defined is the droplet size ratio (D_{ratio}), viz. $D_{ratio}= D_{FFD}/ D_{IFD}$.

2.3 Experimental Methodology

The capillary tubing was used as microchannels (IDEX-Health & Science, USA, part number: 1507 PFA tubing) with inner diameter 1.00 mm and outer diameter 1.50 mm. A 4-junction assembly (P-722, IDEX, USA) was used as a flow-focusing device for the droplet formation. Figure 1a shows the schematic of the microchannels assembled with the 4-Junction assembly.

ACCEPTED MANUSCRIPT

Microchannels were connected to a 4-junction assembly for droplet generation (Figure 1). The schematic of the experimental setup for the droplet control is shown in Figure 2. Two opposite ends of the 4-junction assembly were used as an inlet for CP (oil) via a Y junction and the third end used as an inlet for the DP (ferrofluid). These two inlets (for CP and DP) were connected to a dual rate syringe pumps (KD Scientific). The syringe pump was used to inject fluids into the microfluidic channel by 5.0 ml syringes (Exmire Luer lock gastight syringe). To avoid backflow of the fluids, a unidirectional valve was used along the inlets to the 4-junction assembly. The end opposite to the ferrofluid inlet was used as the outlet (Figure 1 and Figure 2). Different flow rate ratios were used for droplet generation. During the experiment, room temperature was maintained at 25 ^{o}C.

High-speed imaging was performed with a Phantom Miro Camera (Model: M320s) coupled with a magnifying lens (Navitar Zoom 6000)[8, 9, 48-51]. Videos were recorded at 30 frames per second and analyzed by ImageJ software. The diameter of the IFD and the FFD were measured by ImageJ software[48, 49]. Measurements were repeated for at least 15 droplets. Average of the measurements denotes the data points and error were determined by the standard error of the mean[52].

The magnetic field (in the y-direction) was applied perpendicular to the droplet flow (in positive x direction) using Nd-Fe-B permanent magnets (Catalog Number: LRM-ND mag1: NB121010, mag2: NB1266, mag3: 10105, mag4: NB633, Lifton Magnets, Singapore) (Figure 1b). Permanent magnets were placed adjacent to the microchannel for the maximum magnetic field strength. The magnetic field strength of the permanent magnets was measured using Gaussmeter (Lakeshore, Model 410) in ±x direction. The geometry differences were not considered explicitly. However, measured net magnetic field gradient is a result of the

ACCEPTED MANUSCRIPT

magnetic field distribution due to various geometries, which takes in account the geometrical effects. Figure 3 shows the magnetic field distribution in ± x direction with the location of the magnet at x=0 mm.

3 Theory and Modeling

Numerical simulations were performed by COMSOL Multiphysics software. A 2D numerical model was developed for the ferrofluid droplet generation in microchannels, using Laminar Two-Phase Level Set method in fluid dynamics module[48, 49]. AC/DC module was used to model the magnetic field[48, 49].Two Phase Level Set interface module was used at low Reynolds number to track the interface between two immiscible liquids (CP and DP). The physics of the interface was solved by the Navier-Stokes equations for the conservation of the momentum and a continuity equation for the conservation of mass. The laminar Two-Phase Flow, Level Set interface simulations were time-dependent. The AC/DC module was used to compute the static magnetic fields, similar to the experimental parameters.

3.1 Model Geometry

The model geometry consisted of a circular channel with an inner diameter of 1.0 mm and length of 150 mm along x and y-direction. An external magnetic field was applied perpendicular to the microchannel. The simulation was performed with a ferrofluid as the DP and oil as the CP. The experimental magnetic and physical properties of the fluids were used for the simulations. A user controlled mesh (maximum element size of 0.1 mm, minimum element size 4.5 x 10^{-4} mm, the total number of element ~ 500) was separately selected for the external magnetic field (air), microchannel (carrier medium) and ferrofluid droplets. A test case was setup, using mineral oil (viscosity 118 mPa.s) and ferrofluid (viscosity of 5mPa.s) at the flow rate ratio of 1.5.

ACCEPTED MANUSCRIPT

3.2 Theory

Equations 1 and 2 were used to describe the magnetic fields[8, 9, 48-51]:

$$\nabla \cdot \boldsymbol{B} = 0 \tag{1}$$

$$\boldsymbol{B} = \mu_0(\boldsymbol{H} + \boldsymbol{M}) = \mu_0(1 + \chi)\boldsymbol{H} = \mu_0\chi_r\boldsymbol{H} = \mu_r\boldsymbol{H} \tag{2}$$

where χ and χ_r indicate the real susceptibility and relative susceptibility of the ferrofluid, respectively. The vectors $\boldsymbol{B}$, $\boldsymbol{H}$ and $\boldsymbol{M}$ indicate the local magnetic flux density, magnetic field strength and magnetization, respectively. μ_0 and μ_r represent the permeability of free space and relative permeability of the material, respectively.

The effect of the magnetic field in ferrofluid is imparted in terms of volume forces. The magnetic body force (F_{mag}) due to the influence of the magnetic field is given by [50, 53],

$$F_{mag} = \mu_0 (M \cdot \nabla)H \tag{3}$$

The effect of the magnetic field on the droplet flow was determined by adding the magnetic body force term in the Navier-Stokes equation, which is given by [8, 9, 49-51, 53],

$$\underbrace{\rho\left(\frac{\partial \boldsymbol{u}}{\partial t} + \boldsymbol{u}.\nabla\boldsymbol{u}\right)}_{\boldsymbol{F_I}} = \underbrace{-\boldsymbol{\nabla}p}_{\boldsymbol{F_p}} + \underbrace{\boldsymbol{\nabla}\cdot[\eta(\nabla\boldsymbol{u} + \nabla\boldsymbol{u}^{\boldsymbol{T}})]}_{\boldsymbol{F_\eta}} + \boldsymbol{F_{mag}} \tag{4}$$

where, ρ is the fluid density, $\boldsymbol{u}$ is the fluid flow velocity, p is the fluid pressure, and η is the dynamic viscosity of the fluid. $\boldsymbol{F_I}$, $\boldsymbol{F_p}$, $\boldsymbol{F_\eta}$ and $\boldsymbol{F_{mag}}$ are the inertial force per unit volume, net force due to pressure per unit volume, viscous force per unit volume and magnetic body force per unit volume, respectively.

Figure 4 shows the simulation and experimental change in the FFD diameter under the influence of an applied magnetic field. The IFDs are generated at the 4 - junction assembly and flow in the positive x direction (Figure 1). The IFD diameter depends on the flow rate ratio and the viscosity of the medium. Droplet coalescence, resulting in the CFD formation was observed

ACCEPTED MANUSCRIPT

in the vicinity of the permanent magnet, near x=0 mm (Figure 4). The release of the FFDs from the CFD occurs in the positive x region.

The drag force on a droplet for low Reynolds number can be expressed as[48, 54],

$$F_d = 3\pi D\eta v\left(\frac{1 + 2\eta/3\eta_{ff}}{1 + \eta/\eta_{ff}}\right) \quad (5)$$

where, η_{ff}, η and v are the ferrofluid viscosity, CP viscosity and velocity of the droplet in the carrier medium, respectively. D is the ferrofluid droplet diameter.

3.3 Droplet Coalescence Under the Influence of an Applied Magnetic Field

Initial ferrofluid droplets (IFD) were generated in a CP of oil by a 4-junction assembly (Figure 1). When a non-uniform magnetic field (Figure 3) was applied to these moving IFDs, coalescence was observed, leading to the formation of a coalesced ferrofluid droplet (CFD) slug (Figure 1b and Figure 4). Droplet coalescence depends on the magnetic volume force and the hydrodynamic force [37]. The magnetic volume force, F_{mag} increases with the increasing magnetic field strength, the gradient in the magnetic field, ferrofluid susceptibility, and volume concentration of the magnetic nanoparticles (MNP). With the increasing ferrofluid droplet diameter, droplet volume increases, leading to the F_{mag} increase. Hydrodynamic force increases with the increasing viscosity of the CP (η), the flow rate of the CP (Q_{oil}) and the flow rate ratio (Q). Figure 1 and Figure 4 describes the 4-jucntion assembly used for the generation of the IFD, formation of the CFD and the release of the FFD. IFD can be seen to combine to form a CFD slug and after merging of several droplets, a FFD was released from the CFD slug. It is evident from both the experiment and the simulation in Figure 4 that the FFD size is larger than the IFD size (simulation results showing the effect of the CP viscosity on IFD and FFD diameter is available in supplementary Figure S1).

ACCEPTED MANUSCRIPT

3.4 Effect of the Magnetic Field Gradient on Droplet Velocity and Formation of FFDs

The formation of the CFD and the release of the FFD is determined by the inertial force term, $\boldsymbol{F_I}$ (equation 4) and the magnetic body force, F_{mag}. In addition to the F_{mag}, the inertial force term also depends on the other force terms on the right-hand side of equation 4, viz., the net force due to pressure (flow rates of the CP and DP) and the viscous force term. The flow rate and the viscosity of the CP and the DP determine the IFD velocity **u** in the inertial force term.

With no magnetic field, the IFDs travel with a velocity **u** (Figure 1). However, under the influence of the magnetic field gradient, the magnetic force acting on the droplets contributes an additional velocity $\pm\Delta\mathbf{v}_m$, which changes the total velocity of the droplets. The gradient in the magnetic field and the location of the droplets determine the acceleration or deceleration of the droplets. The ± sign indicates the positive and negative $\Delta\mathbf{v}_m$ contribution in the region x<0 and x>0, respectively. $\Delta\mathbf{v}_m$ is positive for the droplets (the IFDs) in the location x<0 due to the attraction of the IFDs towards the magnet, which is along the direction of the flow for x<0. $\Delta\mathbf{v}_m$ is negative for the droplets (the FFDs) in the location x>0 due to the attraction of the droplets towards the magnet, which is opposite to the direction of the flow for x>0.

To explain this further, Figure 5 shows the field gradient along the x-direction that varies from positive to negative with zero slopes at the center. For x= -125 to 0 mm, the droplet accelerates to the center of the magnet and for x= 0 to 125 mm droplet decelerate. When a magnetic field is applied, the first droplet accelerates from negative x and then come to rest near x=0 mm due to F_{mag}. The second IFD follows a similar trend, which now accelerates and coalesces with the initial droplet near x=0 mm, resulting in the formation of the CFD. This process continues until the inertial force ≤ magnetic volume force, resulting in the CFD size increase (Figure 4e-iii). When the inertial force becomes higher than the

ACCEPTED MANUSCRIPT

magnetic volume force ($F_I > F_{mag}$), neck formation and neck elongation takes place. When inertial force dominates the magnetic force ($F_I \gg F_{mag}$), the hydrodynamic force exceeds the magnetic volume force, resulting in a FFD release from the CFD which travels in the positive x direction.

To investigate the effect of droplet size, the ratio Q_{oil}/Q_{ff} was increased, it can be seen from Figure 6 that the droplet size was significantly reduced. Simulations were performed by varying the velocity ratio of the droplet and carrier fluid [55]. For a constant droplet velocity, droplet size decreased as the carrier fluid velocity was increased.

4 Results and Discussion

The microchannel assembled with the 4-Junction assembly (Figure 1a) allows the generation of the IFD in the CP of oil. Flow rate ratio, viscosity, interfacial tension and the inner diameter of the microchannels influence the IFD size [6, 48, 56]. Figure 6 shows the experimentally observed variation in the IFD diameter with the flow rate ratio, Q. With increasing Q, the IFD diameter decreases for both the CPs viz., silicone oil and heavy mineral oil. The IFD diameter also decreases with increasing viscosity of the CP. Smaller IFD size was observed for mineral oil at all flow rate ratio, as compared to the CP of the silicone oil. The change in the IFD diameter shows higher dependence on the flow rate ratio than on the viscosity of the CP [57].

The FFD size can be controlled by an applied magnetic field (Figure 1b). The FFD diameter can also be tuned by changing Q_{oil}, Q_{ff} and the viscosity of the CP. Following sections discuss the effect of an applied magnetic field and flow rate ratios on the FFD size.

ACCEPTED MANUSCRIPT

4.1 Effect of the Magnetic Field at a Constant Flow Rate Ratio

Figure 7 shows the effect of the magnetic field on the FFD size at various flow rate ratios. The FFD size increases with increasing *H* for a fixed Q. Even a small magnetic field can be utilized to induce a significant change in the FFD diameter. Above 10 mT, droplet diameter shows a flattening of the FFD diameter variation. The change in the slope after 10 mT is a combined effect of (i) saturation magnetization and (ii) magnetic volume force. Magnetic volume force and IFD volume determine the FFD volume. Since the saturation magnetization follows the Langevin law, the magnetic volume force also follows the same. The magnetic volume force also depends on the droplet volume. Droplets generated by the flow focusing geometry follows a non-linear behavior. Hence, the combined effect is the change in the slope after 10 mT.

The increase in the FFD diameter was relatively higher for lower viscosity the CP than that for higher viscosity. The FFD diameter is ~2 times the IFD diameter at higher viscosity CP and ~3 times the IFD diameter for lower viscosity CP (Figure 7 and Figure 10a). Higher FFD diameter at a lower viscosity of the CP is due to the less drag force of the lower CP on the ferrofluid droplet, as compared to higher viscosity CP. The magnetic volume force dominates at less drag force, resulting in a larger diameter of the FFD.

The FFD diameter decreases if we increase Q under an applied magnetic field (Figure 8). According to the equation 5, drag force increases with increasing velocity v. Increase in Q, results in the increase in the velocity v and hence increases the drag force. Hence, the growth of the CFD gets reduced due to the increased hydrodynamic force than the magnetic volume force, resulting in the smaller FFD diameter.

Hence, decreasing the flow rate ratio and the viscosity increases the FFD size with increasing magnetic field *H*.

ACCEPTED MANUSCRIPT

4.2 Effect of the Flow Rate Ratio at a Constant Magnetic Field

Experiments were performed with heavy mineral oil and silicone oil in a range of flow rate ratios to investigate the effect of flow rate ratio. At an applied magnetic field *H*, a decrease in the FFD diameter (Figure 9) was observed by changing the viscosity and the flow rate of the CP. It was found that at a constant magnetic field, the FFD diameter decreases with an increase in the viscosity of the CP. At all magnetic fields, the FFD diameter for silicone oil (Figure 9b) is higher than the FFD diameter for heavy mineral oil (Figure 9a). Both silicone oil and heavy mineral oil, show higher FFD diameter profiles at 52 mT than the profiles at H≤34 mT.

Increasing *H* results in a decrease in the FFD size for a given Q and viscosity of the CP. The surface drag of the CP affects the droplet formation. For a constant flow rate, the surface drag force (equation 5) of the medium increases with increasing viscosity. The critical magnetic volume force required for the FFD formation increases at higher viscosity, resulting in a smaller FFD diameters at higher viscosity compared to a low viscosity CP.

4.3 The FFD Size Compared to the IFD Size

The FFD size with respect to the IFD size was analyzed by the droplet size ratio (D_{ratio}), which is the ratio of the FFD diameter to the IFD diameter. Figure 10a and Figure 10b show the effect of the magnetic field and the flow rate ratio on the D_{ratio}, respectively.

At a constant Q, the D_{ratio} increases with increasing magnetic field for both CPs viz., heavy mineral oil and silicone oil (Figure 10a). Highest D_{ratio} of ~3 was observed for silicone oil at the flow rate ratio of 40. Lowest D_{ratio} of ~2 was observed for mineral oil and silicone oil at the flow rate ratio of 10. Silicone oil demonstrated a broad range of D_{ratio} variation, as compared to heavy mineral oil. Intermediate D_{ratio} variation was observed for heavy mineral oil.

At a constant *H*, D_{ratio} increases with Q for both CPs (Figure 10b). Highest D_{ratio} variation with increasing Q, was observed for silicone oil at 52 mT. Minimum D_{ratio} variation

ACCEPTED MANUSCRIPT

with increasing Q, was observed for heavy mineral oil at 6.5 mT. The general behavior of higher D_{ratio} variation with increasing Q, at the higher magnetic fields, was not followed for both CPs at 22 mT, which showed higher D_{ratio} profile than the profiles at 34 mT. All silicone oil profiles showed higher D_{ratio} variation with the increasing Q, as compared to the profiles for heavy mineral oil.

Hence, silicone oil exhibited a broad range of D_{ratio} variation i.e., the ability to tune the FFD size by tuning the magnetic field and flow rate ratio.

5 Discussion

The observed nonlinear trends for silicone oil and heavy mineral oil are the result of four competing forces described in equation 4, i.e., inertial force per unit volume F_I, the net force due to pressure per unit volume F_p, viscous force per unit volume F_η, and magnetic volume force F_{mag}.

The magnetic volume force depends on the droplet volume and susceptibility of the magnetic fluid. For a flow focusing geometry, the droplet size follows a non-linear trend with increasing flow rate ratio, which is evident from Figure 6. Fu et al.[58] and Nie et al.[59] discussed such nonlinear effects in the droplet size due to the flow focusing geometry. The magnitude of this non-linear droplet size increase depends on the flow focusing geometry, the outlet microchannel size, and viscosities of the CP, DP[58, 59]. Also, the magnetic fluid susceptibility follows the Langevin law, which is also nonlinear leading to a nonlinear response to an applied magnetic field. Wu et al. [60] and Varma et al. [48, 61] reported nonlinear droplet size variation under an applied magnetic field.

Hence, the nonlinear trends followed for the IFD size and magnetic volume force are responsible for the non-linear trends observed for the FFD size[48, 60, 61].

ACCEPTED MANUSCRIPT

Droplet tagging, sorting, counting, merging, washing and detection are required for a range of LoC based applications[62-64], these capabilities are offered by magnetically tagged droplet libraries[46, 61, 65]. Tuning the magnetic properties of droplets is advantageous, since it offers selective magnetic tagging as well as selective magnetic response of individual droplets. Based on the magnetic properties, individual droplets can be sorted, counted and detected. The re-pumping mechanism demonstrated in this article offers control of the droplet size after the droplet merging (the FFD) and thus control of the magnetic response. Specifically, merging and magnetic tagging of droplets are useful for LoC based multiplexed sensing applications such as biochemical sensing for luminol-based chemiluminescence blood detection[66], a biochemical assay for measuring glucose in human serum at physiologically relevant levels[67], and multiplex protein detection [68]. Perhaps, the most promising application of the present method can be in magnetic immuno-agglutination assays[69, 70] when combined with a GMR-based magnetofluidic device [71].

Modifying the surfactant matrix surrounding MNPs is a challenge, however, such modifications offer opportunities to encapsulate detection reagents or fluorescent tags. Such combinations result in a complete package for LoC based biochemical detection. If BSA is used in the form of the matrix around the MNPs then it will enhance the biocompatibility useful for the detection of very sensitive samples like human cells[72].

6 Conclusion

The application of external magnetic fields allows selective and controllable manipulation of individual ferrofluid droplets. On-demand changes in droplet diameter can be produced by an external magnetic field. A change in droplet diameter can be induced in droplets flowing across a magnetic field of a permanent magnet. Under the influence of an applied magnetic field, the droplet diameter increased by three times than the initial diameter. This

ACCEPTED MANUSCRIPT

change in droplet diameter, by coalescence of multiple droplets, is advantageous for shear force sensitive substances. The change in the droplet diameter with magnetic field intensity, continuous phase viscosity, initial droplet size and flow rate ratio was studied. This change in the droplet size is relatively higher for a low viscous continuous phase when compared to a high viscous continuous phase under the influence of an applied magnetic field. Manipulation of the magnetic droplet size can be influenced significantly by a low viscous carrier medium and small initial droplet size under a high magnetic field strength. These results can be used to develop wireless technologies in microfluidic applications such as on-demand manipulation and actuation of droplets, transport, mixing, merging, targeted delivery and release for Janus particle synthesis, smart microgel synthesis, immunoassay, chemical, biochemical reactions and cell trapping.

Acknowledgement

The authors are grateful to the SERC, Singapore for financial support for this work through ASTAR PSF 2012 Project: 1321202078.

References

[1] A. Gunther, K.F. Jensen, Multiphase microfluidics: from flow characteristics to chemical and materials synthesis, Lab Chip, 6(2006) 1487-503.

[2] G. Korir, M. Prakash, Punch card programmable microfluidics, PLoS One, 10(2015) e0115993.

[3] J.K. Nunes, S.S. Tsai, J. Wan, H.A. Stone, Dripping and jetting in microfluidic multiphase flows applied to particle and fiber synthesis, Journal of physics D: Applied physics, 46(2013) 114002.

[4] C. Rivet, H. Lee, A. Hirsch, S. Hamilton, H. Lu, Microfluidics for medical diagnostics and biosensors, Chemical Engineering Science, 66(2011) 1490-507.

[5] J. Wu, W. Wen, P. Sheng, Smart electroresponsive droplets in microfluidics, Soft Matter, 8(2012) 11589.

[6] J.D. Tice, H. Song, A.D. Lyon, R.F. Ismagilov, Formation of droplets and mixing in multiphase microfluidics at low values of the Reynolds and the capillary numbers, Langmuir, 19(2003) 9127-33.

ACCEPTED MANUSCRIPT

[7] H. Song, D.L. Chen, R.F. Ismagilov, Reactions in droplets in microfluidic channels, Angewandte chemie international edition, 45(2006) 7336-56.

[8] Z.M. Wang, V.B. Varma, H.M. Xia, Z.P. Wang, R.V. Ramanujan, Spreading of a ferrofluid core in three-stream micromixer channels, Physics of Fluids, 27(2015) 052004.

[9] Z.M. Wang, V.B. Varma, Z.P. Wang, R.V. Ramanujan, Tuning magnetofluidic spreading in microchannels, Journal of Micromechanics and Microengineering, 25(2015) 124001.

[10] I. Jang, S. Song, Facile and precise flow control for a paper-based microfluidic device through varying paper permeability, Lab Chip, 15(2015) 3405-12.

[11] S. Zeng, B. Li, X. Su, J. Qin, B. Lin, Microvalve-actuated precise control of individual droplets in microfluidic devices, Lab Chip, 9(2009) 1340-3.

[12] Z.Z. Chong, S.H. Tan, A.M. Ganan-Calvo, S.B. Tor, N.H. Loh, N.T. Nguyen, Active droplet generation in microfluidics, Lab Chip, 16(2016) 35-58.

[13] C.N. Baroud, F. Gallaire, R. Dangla, Dynamics of microfluidic droplets, Lab Chip, 10(2010) 2032-45.

[14] U. Tangen, A. Sharma, P. Wagler, J.S. McCaskill, On demand nanoliter-scale microfluidic droplet generation, injection, and mixing using a passive microfluidic device, Biomicrofluidics, 9(2015) 014119.

[15] T.J. Johnson, D. Ross, L.E. Locascio, Rapid Microfluidic Mixing, Analytical Chemistry, 74(2002) 45-51.

[16] Y.K. Suh, S. Kang, A Review on Mixing in Microfluidics, Micromachines, 1(2010) 82-111.

[17] C.-Y. Lee, C.-L. Chang, Y.-N. Wang, L.-M. Fu, Microfluidic Mixing: A Review, International Journal of Molecular Sciences, 12(2011) 3263.

[18] S. Balasuriya, Dynamical systems techniques for enhancing microfluidic mixing, J Micromech Microeng, 25(2015) 094005.

[19] A. Winkler, S. Harazim, S. Menzel, H. Schmidt, SAW-based fluid atomization using mass-producible chip devices, Lab on a chip, 15(2015) 3793-9.

[20] L.D. Garza-Garcia, E. Garcia-Lopez, S. Camacho-Leon, M. Del Refugio Rocha-Pizana, F. Lopez-Pacheco, J. Lopez-Meza, et al., Continuous flow micro-bioreactors for the production of biopharmaceuticals: the effect of geometry, surface texture, and flow rate, Lab Chip, 14(2014) 1320-9.

[21] S.H. Tan, B. Semin, J.C. Baret, Microfluidic flow-focusing in ac electric fields, Lab Chip, 14(2014) 1099-106.

[22] J. Zeng, Non-linear electrohydrodynamics in microfluidic devices, Int J Mol Sci, 12(2011) 1633-49.

[23] J.D. Wehking, R. Kumar, Droplet actuation in an electrified microfluidic network, Lab on a chip, 15(2015) 793-801.

ACCEPTED MANUSCRIPT

[24] A. Ray, T.M. Fischer, Magnetic field controlled composite paramagnetic-diamagnetic colloidal phases, J Phys Chem B, 116(2012) 8233-40.

[25] A. Ray, S. Aliaskarisohi, T.M. Fischer, Dynamics of self-assembly of flower-shaped magnetic colloidal clusters, Phys Rev E Stat Nonlin Soft Matter Phys, 82(2010) 031406.

[26] A. Ray, T.M. Fischer, The transition strength from solid to liquid colloidal dipolar clusters in precessing magnetic fields, Eur Phys J E Soft Matter, 35(2012) 1-6.

[27] K. Zhang, Q. Liang, X. Ai, P. Hu, Y. Wang, G. Luo, On-demand microfluidic droplet manipulation using hydrophobic ferrofluid as a continuous-phase, Lab on a chip, 11(2011) 1271-5.

[28] H. Gu, M.H. Duits, F. Mugele, Droplets formation and merging in two-phase flow microfluidics, Int J Mol Sci, 12(2011) 2572-97.

[29] G.F. Christopher, S.L. Anna, Microfluidic methods for generating continuous droplet streams, Journal of physics D: Applied physics, 40(2007) R319-R36.

[30] T. Zhu, R. Cheng, G.R. Sheppard, J. Locklin, L. Mao, Magnetic-Field-Assisted Fabrication and Manipulation of Nonspherical Polymer Particles in Ferrofluid-Based Droplet Microfluidics, Langmuir, 31(2015) 8531-4.

[31] K. Raj, B. Moskowitz, R. Casciari, Advances in ferrofluid technology, Journal of magnetism and magnetic materials, 149(1995) 174-80.

[32] O. Marinică, D. Susan-Resiga, F. Bălănean, D. Vizman, V. Socoliuc, L. Vékás, Nano-micro composite magnetic fluids: Magnetic and magnetorheological evaluation for rotating seal and vibration damper applications, Journal of Magnetism and Magnetic Materials, 406(2016) 134-43.

[33] W. Huang, X. Wang, Ferrofluids lubrication: a status report, Lubrication Science, 28(2016) 3-26.

[34] A. Sudarsan, M.G. Pollack, P. Thwar, D. Allen, Bead manipulations on a droplet actuator, Google Patents2013.

[35] A. Beyzavi, N.-T. Nguyen, One-dimensional actuation of a ferrofluid droplet by planar microcoils, Journal of Physics D: Applied Physics, 42(2008) 015004.

[36] R. Seemann, M. Brinkmann, T. Pfohl, S. Herminghaus, Droplet based microfluidics, Reports on progress in physics, 75(2011) 016601.

[37] N.T. Nguyen, K.M. Ng, X.Y. Huang, Manipulation of ferrofluid droplets using planar coils, Applied Physics Letters, 89(2006) 052509.

[38] N.-T. Nguyen, Z. Wu, Micromixers—a review, Journal of Micromechanics and Microengineering, 15(2004) R1.

[39] N. Pamme, Magnetism and microfluidics, Lab on a chip, 6(2006) 24-38.

[40] L.M. Fidalgo, C. Abell, W.T.S. Huck, Surface-induced droplet fusion in microfluidic devices, Lab on a chip, 7(2007) 984-6.

[41] W. Wang, C. Yang, C.M. Li, On-demand microfluidic droplet trapping and fusion for on-chip static droplet assays, Lab on a chip, 9(2009) 1504-6.

ACCEPTED MANUSCRIPT

[42] W. Wang, C. Yang, Y. Liu, C.M. Li, On-demand droplet release for droplet-based microfluidic system, Lab on a chip, 10(2010) 559-62.

[43] S.H. Tan, B. Semin, J.-C. Baret, Novel Electrical Control in Droplet Microfluidics Using an AC Electric Field, ASME 2013 11th International Conference on Nanochannels, Microchannels, and Minichannels, American Society of Mechanical Engineers2013, pp. V001T03A-VT03A.

[44] D.R. Link, E. Grasland-Mongrain, A. Duri, F. Sarrazin, Z. Cheng, G. Cristobal, et al., Electric Control of Droplets in Microfluidic Devices, Angewandte Chemie International Edition, 45(2006) 2556-60.

[45] W. Shi, J. Qin, N. Ye, B. Lin, Droplet-based microfluidic system for individual Caenorhabditis elegans assay, Lab on a chip, 8(2008) 1432-5.

[46] G. Katsikis, J.S. Cybulski, M. Prakash, Synchronous universal droplet logic and control, Nature Physics, 11(2015) 588-96.

[47] S. Kahkeshani, D. Di Carlo, Drop formation using ferrofluids driven magnetically in a step emulsification device, Lab on a chip, 16(2016) 2474-80.

[48] V.B. Varma, A. Ray, Z. Wang, Z. Wang, R. Wu, P.J. Jayaneel, et al., Control of Ferrofluid Droplets in Microchannels by Uniform Magnetic Fields, IEEE Magnetics Letters, 7(2016) 1-5.

[49] A. Ray, V.B. Varma, Z. Wang, P.J. Jayaneel, N.M. Sudharsan, R.V. Ramanujan, Magnetic Droplet Merging by Hybrid Magnetic Fields, IEEE Magnetics Letters, PP(2016) In Press.

[50] X. Wang, Z. Wang, V.B. Varma, Z. Wang, A. Ray, W.S. Lew, et al., Instability-Induced Mixing of Ferrofluids in Uniform Magnetic Fields, IEEE Magnetics Letters, PP(2016) In Press.

[51] Z.M. Wang, R.G. Wu, Z.P. Wang, R.V. Ramanujan, Magnetic Trapping of Bacteria at Low Magnetic Fields, Sci Rep, 6(2016) 26945.

[52] M.L. Boas, Mathematical methods in the physical sciences, 3 ed.: Wiley New York; 2006.

[53] R.E. Rosensweig, Ferrohydrodynamics: Dover Publications, Inc. New York; 2013.

[54] F.M. White, I. Corfield, Viscous fluid flow: McGraw-Hill New York; 2006.

[55] A. Abrishamkar, A.S. Rane, K.S. Elvira, R.C.R. Wootton, T. Sainio, A.J. deMello, A COMSOL Multiphysics® Model of Droplet Formation at a Flow Focusing Device, COMSOL Conference, Rotterdam-2013.

[56] D. Pan, N. Phan-Thien, B.C. Khoo, Dissipative particle dynamics simulation of droplet suspension in shear flow at low Capillary number, Journal of Non-Newtonian Fluid Mechanics, 212(2014) 63-72.

[57] T. Cubaud, T.G. Mason, Capillary threads and viscous droplets in square microchannels, Physics of Fluids (1994-present), 20(2008) 053302.

[58] T. Fu, Y. Wu, Y. Ma, H.Z. Li, Droplet formation and breakup dynamics in microfluidic flow-focusing devices: from dripping to jetting, Chemical engineering science, 84(2012) 207-17.

ACCEPTED MANUSCRIPT

[59] Z. Nie, M. Seo, S. Xu, P.C. Lewis, M. Mok, E. Kumacheva, et al., Emulsification in a microfluidic flow-focusing device: effect of the viscosities of the liquids, Microfluidics and Nanofluidics, 5(2008) 585-94.

[60] Y. Wu, T. Fu, Y. Ma, H.Z. Li, Ferrofluid droplet formation and breakup dynamics in a microfluidic flow-focusing device, Soft Matter, 9(2013) 9792-8.

[61] V.B. Varma, A. Ray, Z.M. Wang, Z.P. Wang, R.V. Ramanujan, Droplet Merging on a Lab-on-a-Chip Platform by Uniform Magnetic Fields, Sci Rep, 6(2016) 37671.

[62] S.Y. Teh, R. Lin, L.H. Hung, A.P. Lee, Droplet microfluidics, Lab on a Chip, 8(2008) 198-220.

[63] T.P. Lagus, J.F. Edd, A review of the theory, methods and recent applications of high-throughput single-cell droplet microfluidics, Journal of Physics D-Applied Physics, 46(2013) 21.

[64] H. Lee, L.F. Xu, K.W. Oh, Droplet-based microfluidic washing module for magnetic particle-based assays, Biomicrofluidics, 8(2014) 10.

[65] J.S. Sander, R.M. Erb, C. Denier, A.R. Studart, Magnetic transport, mixing and release of cargo with tailored nanoliter droplets, Adv Mater, 24(2012) 2582-7, 10.

[66] V. Nock, Y. Muller, M. Sellier, C. Verdier, Biochemical sensing assays based on coalescence-induced self-propulsion digital microfluidics, Sensing Technology (ICST), 2013 Seventh International Conference on2013, pp. 67-70.

[67] B. Hadwen, G.R. Broder, D. Morganti, A. Jacobs, C. Brown, J.R. Hector, et al., Programmable large area digital microfluidic array with integrated droplet sensing for bioassays, Lab on a Chip, 12(2012) 3305-13.

[68] D. Han, J.K. Park, Microarray-integrated optoelectrofluidic immunoassay system, Biomicrofluidics, 10(2016) 9.

[69] B. Teste, A. Ali-Cherif, J.L. Viovy, L. Malaquin, A low cost and high throughput magnetic bead-based immuno-agglutination assay in confined droplets, Lab Chip, 13(2013) 2344-9.

[70] H.C. Tekin, M.A. Gijs, Ultrasensitive protein detection: a case for microfluidic magnetic bead-based assays, Lab on a Chip, 13(2013) 4711-39.

[71] G.G. Lin, V.M. Fomin, D. Makarov, O.G. Schmidt, Supervised discriminant analysis for droplet micro-magnetofluidics, Microfluidics and Nanofluidics, 19(2015) 457-64.

[72] M.D. Krebs, R.M. Erb, B.B. Yellen, B. Samanta, A. Bajaj, V.M. Rotello, et al., Formation of ordered cellular structures in suspension via label-free negative magnetophoresis, Nano letters, 9(2009) 1812-7.

ACCEPTED MANUSCRIPT

Author Biographies

Dr. Ayan Ray has obtained his integrated M.Sc. from Department of Physics, Indian Institute of Technology Kharagpur India. He went on to receive his PhD in the field of experimental physics from the University of Bayreuth, Germany. He is currently carrying out his research in Nanyang Technological University, Singapore. His research interest is focus on microfluidics, magnetic nanomaterials, thin films, soft matter and characterization techniques.

Mr. Vijaykumar B. Varma has obtained his M.Sc. from Department of Physics, University of Pune, India. Presently he is carrying his doctoral studies at Nanyang Technological University, Singapore. His research includes droplet microfluidics, micro-magnetofluidics, COMSOL, nanomaterials, protein detection, Janus particles synthesis, and characterization.

Mr. P. J. Jayaneel is working as a researcher in the Department of Mechanical Engineering, Rajalakshmi Engineering College, India. His research includes microfluidics, COMSOL and computational fluid dynamics.

Prof. Natteri M. Sudharsan has obtained his M.Sc. from California State University-Sacramento, U.S.A and PhD from Nanyang Technological University, Singapore. He is presently Professor in the department of Mechanical engineering at Rajalakshmi Engineering College, India. His research interest includes computational fluid dynamics, microfluidics, heat transfer and numerical analysis.

Dr. Zhiping Wang obtained his M.Sc. from Nanjing University of Aeronautics and Astronautics, China and PhD from Oxford University, UK. He is currently at Singapore Institute of Manufacturing Technology, Singapore. His research interests include manufacturing, manufacturing process, microfluidics and microfabrication.

ACCEPTED MANUSCRIPT

Prof. Raju V. Ramanujan, FASM, is currently at the School of Materials Science and Engineering, Nanyang Technological University, Singapore. He obtained his Master of Engineering and Ph.D. degrees from the Department of Materials Science and Engineering, Carnegie Mellon University, Pittsburgh, U.S.A. His research interests include the study and development of advanced nanomaterials, especially magnetic and multifunctional nanomaterials, magnetocaloric materials, hard magnetic nanomaterials, "smart" magnet based composites, and magnetic Janus particles for a variety of energy, bioengineering, transducer, microfluidics and Lab-on-a-Chip applications.

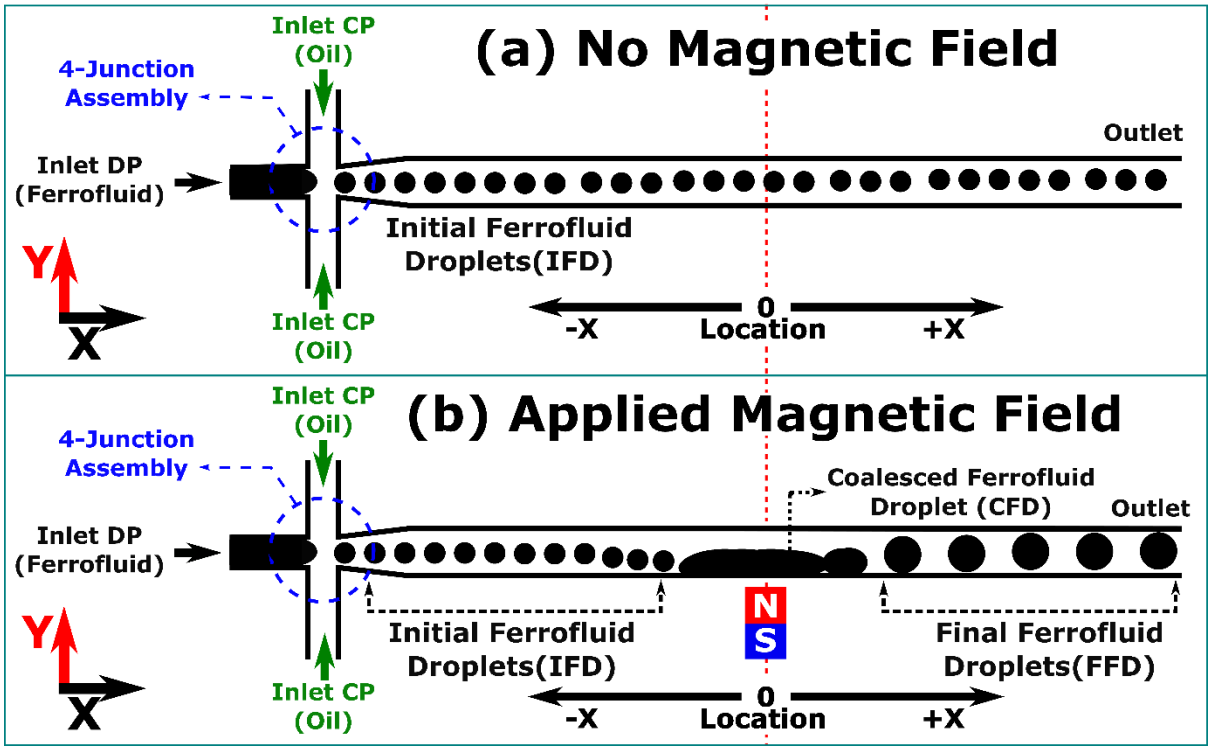

Figure 1. Schematic of (a) initial ferrofluid droplet (IFD) generation by a 4-Junction assembly with no magnetic field and (b) effect of an applied magnetic field on IFDs resulting in the formation of the final ferrofluid droplets (FFD). A permanent magnet was used to apply the magnetic field. Center of the magnet was selected as the reference location x=0, denoted by the dotted red line. In the negative x region (x<0), IFD are generated. Near x=0, IFDs coalesce and the formation of a coalesced ferrofluid droplet (CFD) takes place. The FFDs are then released from the CFD, with a larger diameter than the IFDs. The diameter of the FFDs can be tuned by the applied magnetic field and the flow rate ratio.

ACCEPTED MANUSCRIPT

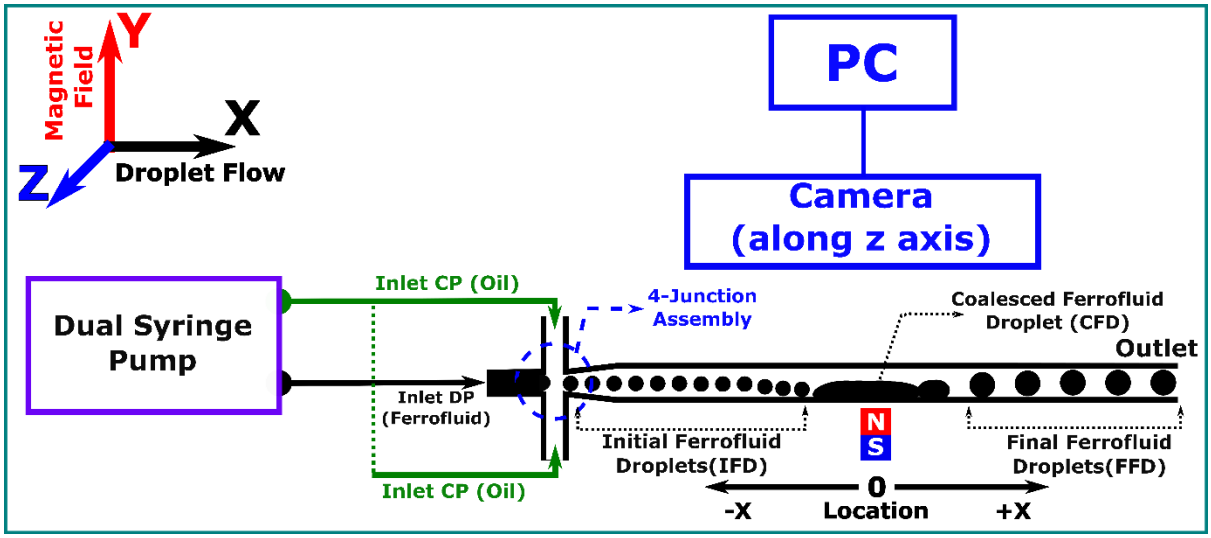

Figure 2. Schematic of the experimental set-up used for the investigation. The dual syringe pump was used to control the flow rates of the continuous phase (CP) of oil and the dispersed phase (DP) of the ferrofluid. Initial ferrofluid droplet (IFD) formation takes place at the 4-junction assembly in the positive x direction. The magnetic field was applied in the y direction. The camera was mounted in the z direction.

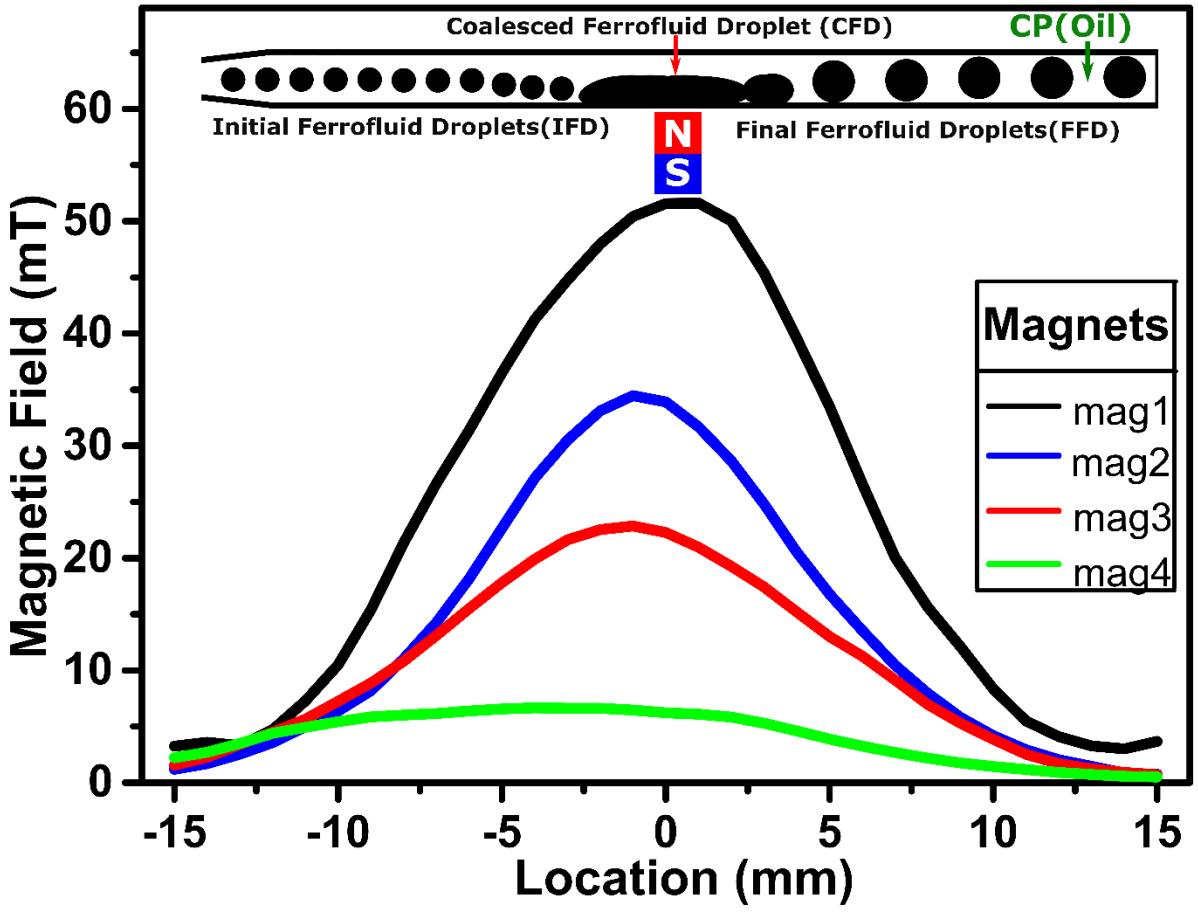

ACCEPTED MANUSCRIPT

Figure 3. Magnetic field distribution of different permanent magnets used for the selective control of the droplets. Center of the magnet was assigned reference location x=0 mm and field distribution was measured in the ±x direction (Figure 1). The magnetic field strength increases for x=-15 to 0 mm and decreases for x=0 to 15 mm. Surface areas of the corresponding permanent magnets are, mag1: 1.0 cm x 1.0 cm, mag2: 0.3 cm x 0.3 cm, mag3: radius = 1.2 cm, and mag4: radius = 1.0 cm.

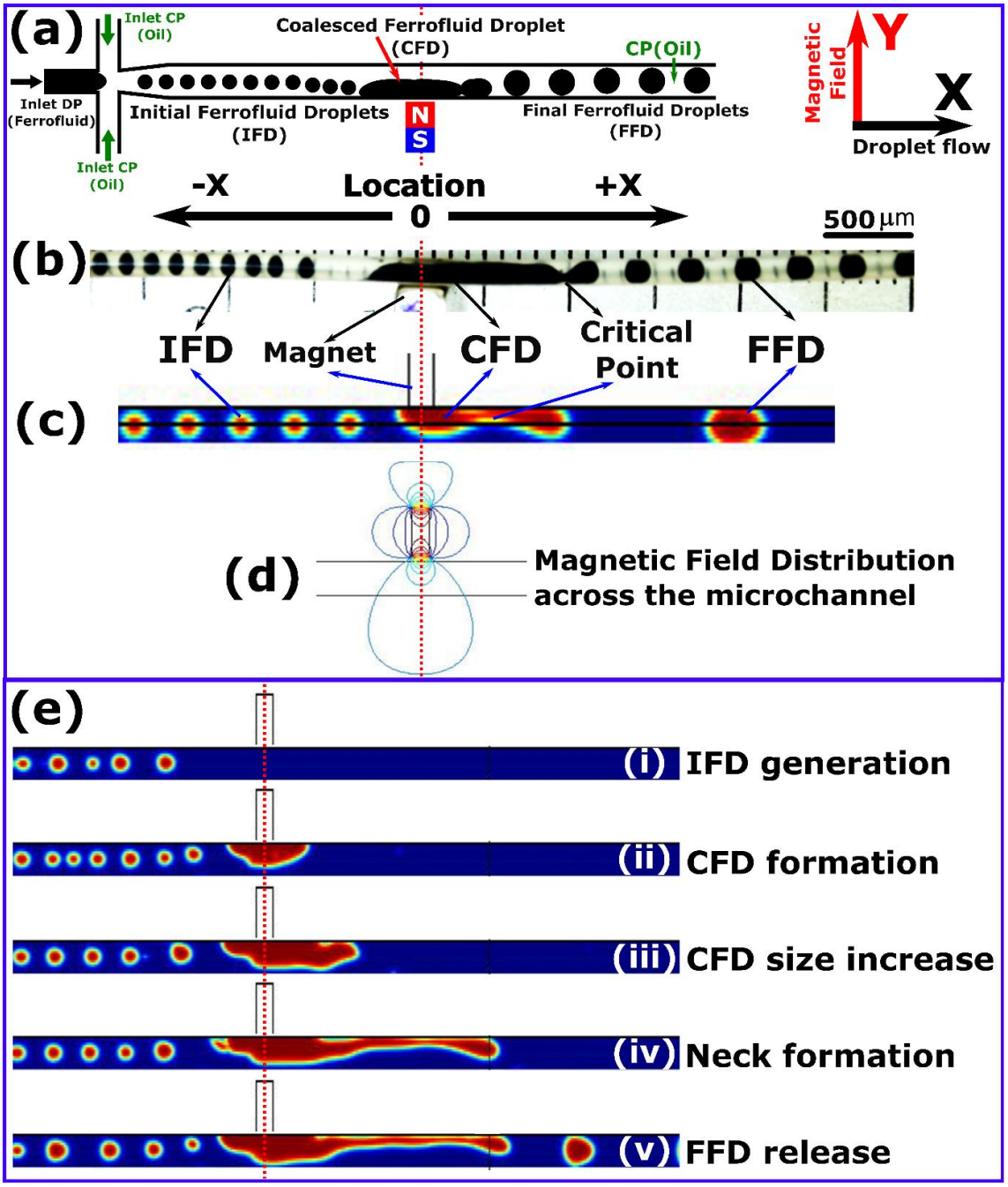

Figure 4. Experimental and simulated formation of the final ferrofluid droplets (FFD) from the initial ferrofluid droplets (IFD): **(a)** schematic; **(b)** experimental IFDs and FFDs; **(c)** simulated IFDs and FFDs; **(d)** simulated magnetic field distribution across the microchannel, responsible for the FFD pinch-off from the CFD (red lines and blue lines denote, high and low magnetic fields, respectively); **(e)** process

ACCEPTED MANUSCRIPT

of the FFD formation from the IFD (i) IFDs accelerate for x<0 due to F_{mag}, (ii) CFD formation by the coalescence of the IFDs near x=0 mm, (iii) increase in the CFD size due to merging of more IFDs, (iv) neck formation in the CFD, (v) release of the FFD of larger size than the IFD size. Where IFDs are generated by the 4-junction assembly. Droplet flow is in the positive x direction. Under the influence of the magnetic field, the CFD forms near x=0 mm due to coalescence of the IFDs. FFDs are then generated from the CFD. The diameter of the FFD is larger than the IFD, which can be tuned by the magnetic field and flow rate ratio. Red dotted line indicates the reference location x= 0 mm, which is the center of the permanent magnet.

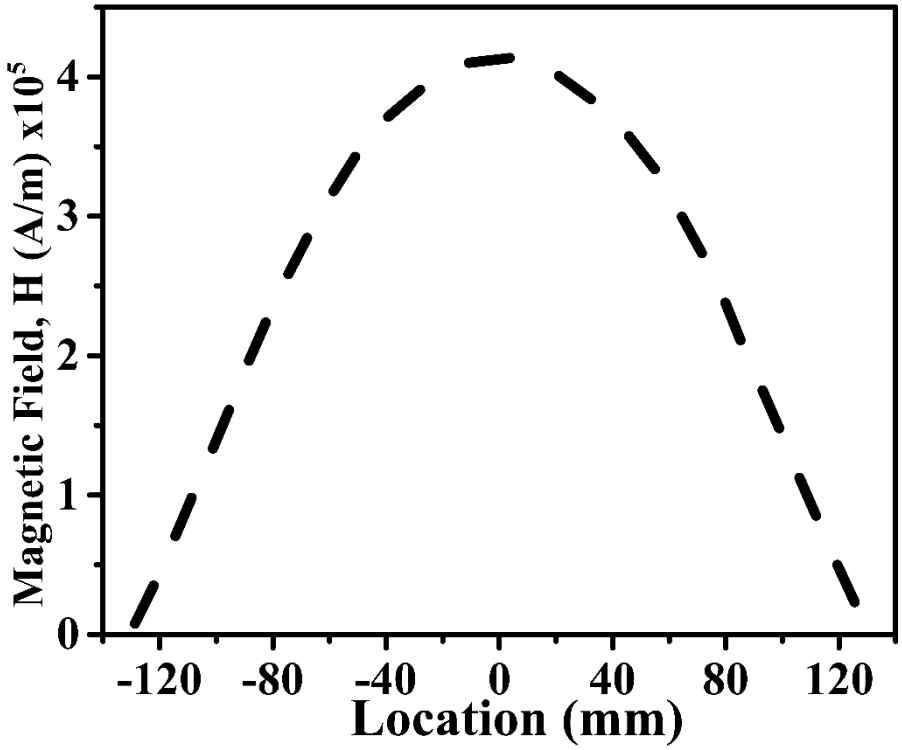

Figure 5. Simulated magnetic field gradient along the microchannel length (x-direction). At 0 mm magnetic field strength is highest (central location of the magnet) and the field strength decreases on both sides of the peak. Droplet accelerates for x= -125 to 0 mm, due to the increasing field gradient and droplet decelerates for x= 0 to 125 mm due to the decreasing field gradient.

ACCEPTED MANUSCRIPT

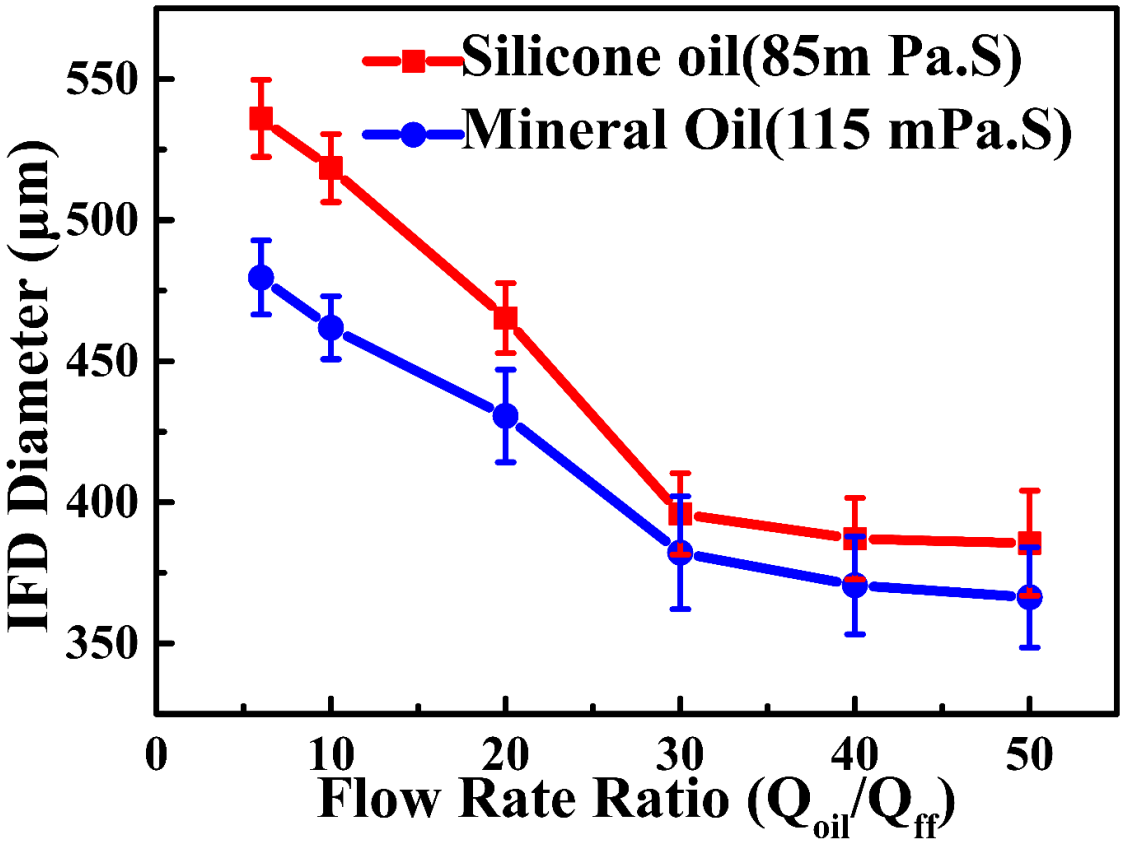

Figure 6. Initial ferrofluid droplet (IFD) diameter variation with flow rate ratio (Q) for the CP of heavy mineral oil and silicone oil, in the absence of magnetic field. Where, $Q=Q_{oil}/Q_{ff}$ for a constant Q_{oil}=5000 µl/h and at Q_{ff} =100, 125, 166, 250, 500, 750 µl/h.

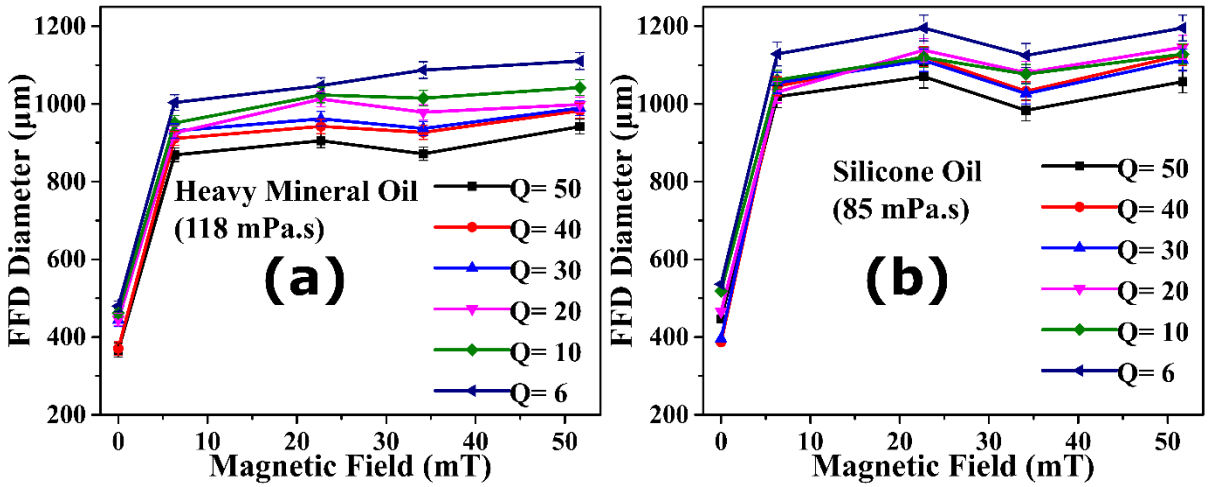

Figure 7. Effect of an applied magnetic field at different Q, on the final ferrofluid droplet (FFD) diameter for the CP of (a) heavy mineral oil and (b) silicone oil. Where, Q was changed from 6 to 50 and H changed from 0 to 52 mT (peak of the magnetic field distribution in Figure 3).

ACCEPTED MANUSCRIPT

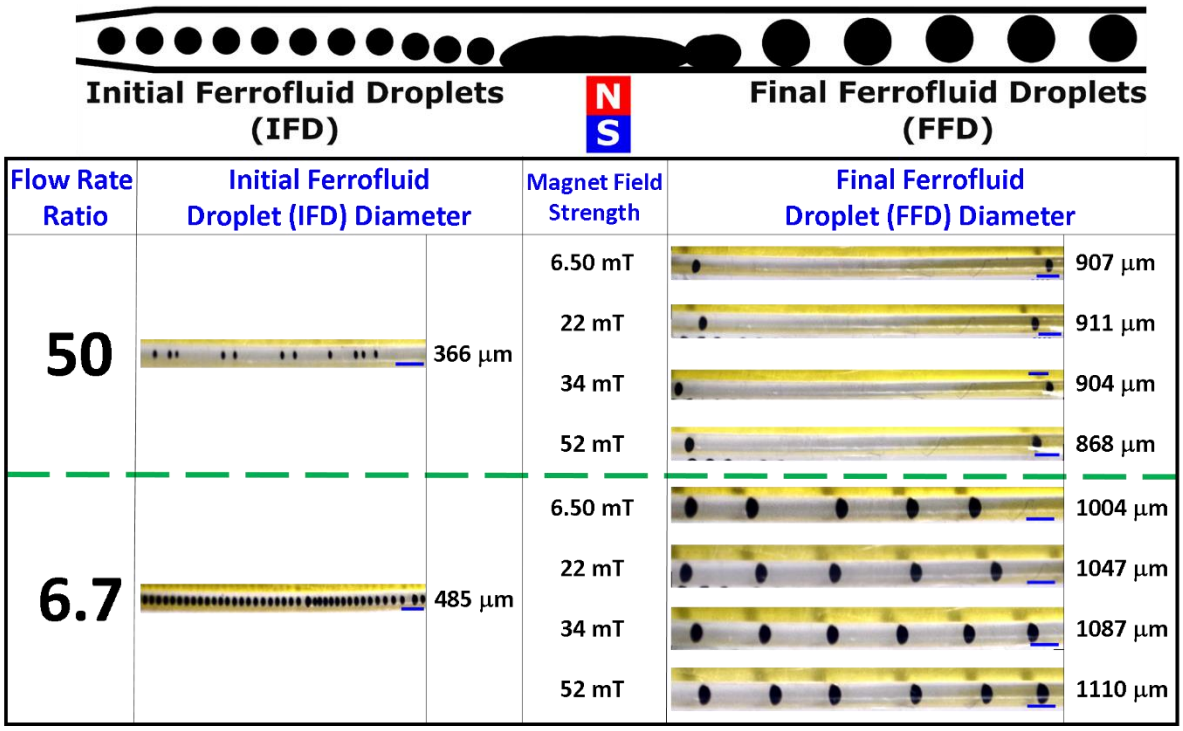

Figure 8. The effect of magnetic field strength on the final ferrofluid droplet (FFD) diameter at Q=6.7, 50 and *H*=6.5, 22, 34, 52 mT: (i) the initial ferrofluid droplet (IFD) diameter in x<0 region and (ii) the FFD diameter in x>0 region (Figure 1b). Where, the magnetic field *H* was applied by a permanent magnet placed at x= 0 mm. Scale bar= 2000 μm.

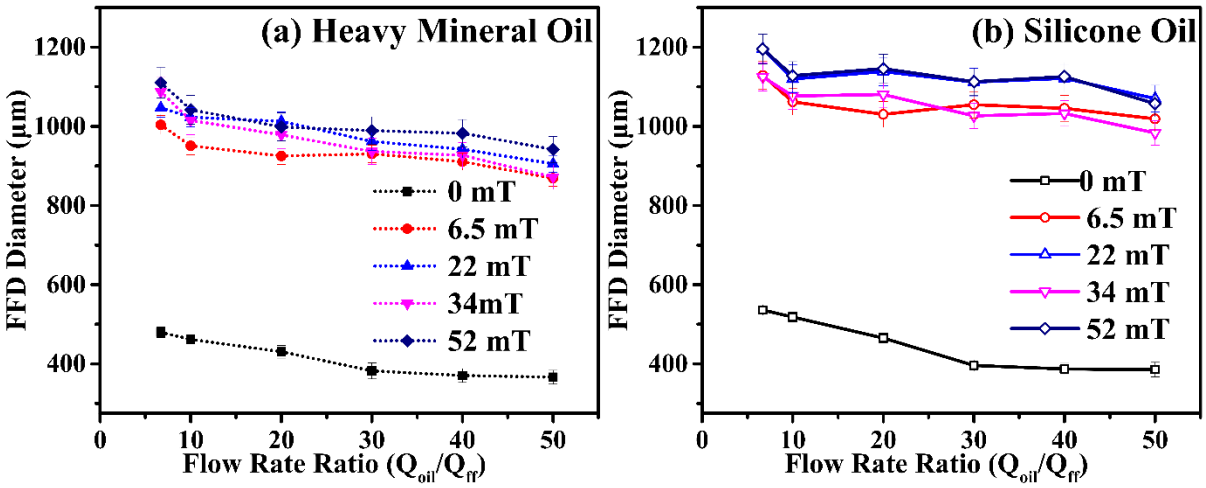

Figure 9. Variation of the final ferrofluid droplet (FFD) diameter with the flow rate ratio, at a constant magnetic field (*H*=0, 6.5, 22, 34, 52 mT) for the CP of (a) heavy mineral oil (HMO, 118 mPa.s) and (b) silicone oil (SO, 85 mPa.s).

ACCEPTED MANUSCRIPT

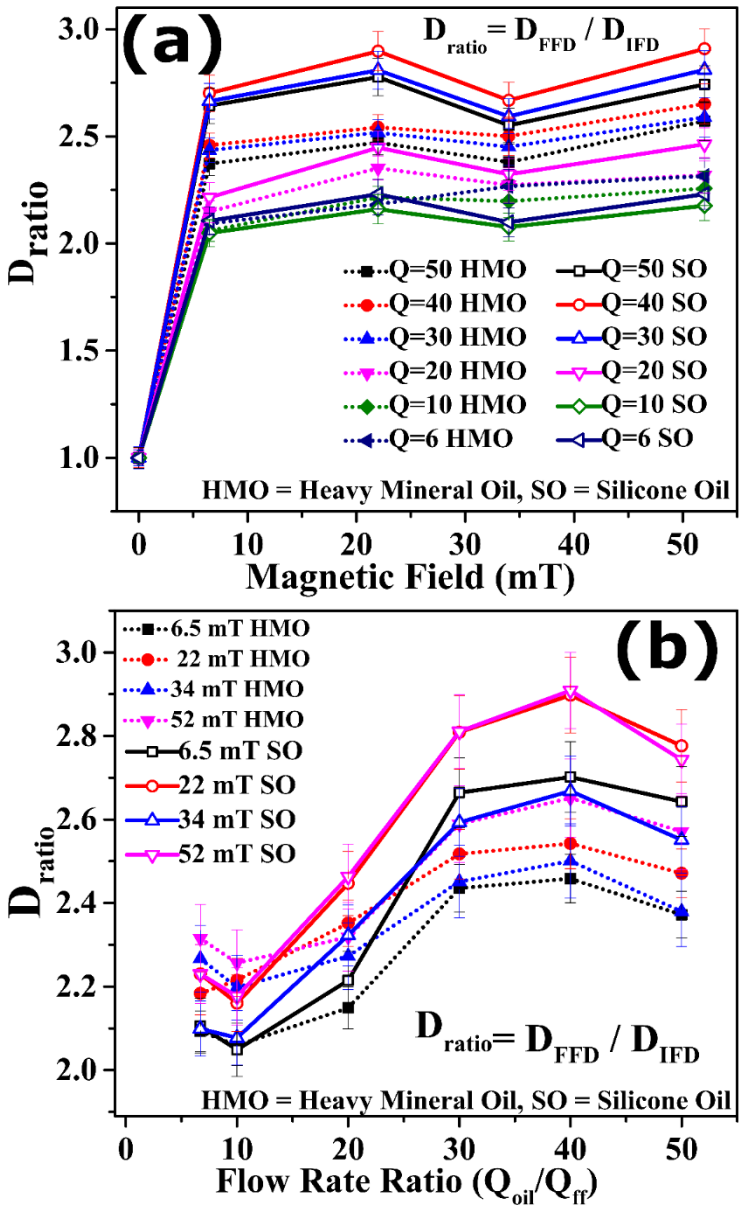

Figure 10. Variation of the D_{ratio} for the CP of heavy mineral oil (HMO) and silicone oil (SO) with (a) magnetic field for Q= 6, 10, 20, 30, 40, 50, and (b) with the flow rate ratio, at *H*=0, 6.5, 22, 34, 52 mT. Where, D_{IFD} and D_{FFD} are the initial ferrofluid droplet (IFD) diameter and the final ferrofluid droplet (FFD) diameter, respectively. $D_{ratio} = D_{FFD}/D_{IFD}$ and $Q= Q_{oil}/Q_{ff}$.